ICES REPORT 11-13

May 2011

On the Nesting Behavior of T-splines

by

X. Li and M. A. Scott

The Institute for Computational Engineering and Sciences
The University of Texas at Austin
Austin, Texas 78712

Reference: X. Li and M. A. Scott, "On the Nesting Behavior of T-splines", ICES REPORT 11-13, The Institute for Computational Engineering and Sciences, The University of Texas at Austin, May 2011.

Report Documentation Page

Form Approved
OMB No. 0704-0188

1. REPORT DATE	2. REPORT TYPE	3. DATES COVERED
MAY 2011		**00-00-2011 to 00-00-2011**

4. TITLE AND SUBTITLE	5a. CONTRACT NUMBER
On the Nesting Behavior of T-splines	5b. GRANT NUMBER
	5c. PROGRAM ELEMENT NUMBER
6. AUTHOR(S)	5d. PROJECT NUMBER
	5e. TASK NUMBER
	5f. WORK UNIT NUMBER
7. PERFORMING ORGANIZATION NAME(S) AND ADDRESS(ES) **University of Texas at Austin,Institute for Computational Engineering and Sciences,Austin,TX,78712**	8. PERFORMING ORGANIZATION REPORT NUMBER
9. SPONSORING/MONITORING AGENCY NAME(S) AND ADDRESS(ES)	10. SPONSOR/MONITOR'S ACRONYM(S)
	11. SPONSOR/MONITOR'S REPORT NUMBER(S)

12. DISTRIBUTION/AVAILABILITY STATEMENT
Approved for public release; distribution unlimited

13. SUPPLEMENTARY NOTES

14. ABSTRACT
We establish rigorously the fundamental nesting behavior of T-spline spaces in terms of the topology of the T-mesh. This provides a theoretical foundation for local refinement algorithms based on analysis-suitable T-splines and their use in isogeometric analysis. A key result is a dimension formula for smooth polynomial spline spaces defined over the B?ezier mesh of a T-spline.

15. SUBJECT TERMS

16. SECURITY CLASSIFICATION OF:			17. LIMITATION OF ABSTRACT	18. NUMBER OF PAGES	19a. NAME OF RESPONSIBLE PERSON
a. REPORT	b. ABSTRACT	c. THIS PAGE			
unclassified	**unclassified**	**unclassified**	**Same as Report (SAR)**	**21**	

On the Nesting Behavior of T-splines

X. Li[a,*], M. A. Scott[b]

[a] *Department of Mathematics, USTC, Hefei, Anhui Province 230026, P. R. China*
[b] *Institute for Computational Engineering and Sciences, The University of Texas at Austin, Austin, Texas 78712, USA*

Abstract

We establish rigorously the fundamental nesting behavior of T-spline spaces in terms of the topology of the T-mesh. This provides a theoretical foundation for local refinement algorithms based on analysis-suitable T-splines and their use in isogeometric analysis. A key result is a dimension formula for smooth polynomial spline spaces defined over the Bézier mesh of a T-spline.

Keywords: T-splines, isogeometric analysis, local refinement, T-spline spaces

1. Introduction

T-splines were originally introduced as a superior alternative to NURBS [1] and have emerged as an important technology across several disciplines including industrial, architectural, and engineering design, manufacturing, and engineering analysis. T-splines can model complicated designs as a single, watertight geometry and can be locally refined [2, 3]. These basic properties make it possible to merge multiple NURBS patches into a single T-spline [4, 1] and any trimmed NURBS model can be represented as a watertight T-spline [5].

T-splines are an ideal discretization technology for isogeometric analysis [6, 7, 3, 8, 9, 10, 11]. Isogeometric analysis was introduced in [12] and described in detail in [13]. The isogeometric paradigm is simple: use the smooth geometric basis as the basis for analysis. Traditional design-through-analysis procedures such as geometry clean-up, defeaturing, and mesh generation are avoided. Additionally, the higher-order smoothness provides substantial gains to analysis in terms of accuracy and robustness of finite element solutions [14, 15].

Analysis-suitable T-splines, a mildly restricted subset of T-splines, are optimized to meet the needs of both design and analysis [16, 3]. Analysis-suitable T-splines maintain the important mathematical properties of NURBS, such as linear independence [16] and partition of unity [17], while providing an efficient and highly localized refinement capability [3].

*Corresponding author
Email address: lixustc@ustc.edu.cn (X. Li)

In this paper we establish rigorously the nesting behavior of analysis-suitable T-splines. This provides the theoretical justification for the analysis-suitable local refinement algorithm in [3] and provides important insights into T-spline spaces in general. A key result is a simple dimension formula for polynomial spline spaces defined over the Bézier mesh of a T-spline [18]. The formula, written only in terms of topological quantities, "bridges the gap" between T-splines and traditional spline spaces posed over partitions of $\mathbb{R}^2$. We feel that this may have important implications in establishing approximation, stability, and error estimates for T-splines in isogeometric analysis [19] by allowing theoretical tools, established for traditional spline spaces, to be used directly for T-spline spaces.

This paper is organized as follows. Section 2 establishes notation and reviews fundamental T-spline concepts. T-junction extensions and the extended T-mesh are then described in Section 3. Section 6 uses the smoothing cofactor-conformality method to develop an algebraic representation of the smoothness properties of a polynomial spline space posed over the Bézier mesh of a T-spline. A dimension formula for these polynomial spline spaces is then derived in Section 7. Finally, Section 8 establishes the nesting behavior of T-spline spaces.

2. T-spline fundamentals

We restrict our developments to cubic T-spline surfaces. All results can be easily generalized to other *odd* polynomial orders.

2.1. The T-mesh

A T-spline is defined in terms of a control grid or *T-mesh*, T, and two *global knot vectors*, $\Xi = [\xi_{-2}, \xi_{-1}, \xi_0, \ldots, \xi_{c+1}, \xi_{c+2}, \xi_{c+3}]$ and $\Pi = [\eta_{-2}, \eta_{-1}, \eta_0, \ldots, \eta_{d+1}, \eta_{d+2}, \eta_{d+3}]$. Interior knots may have a multiplicity of three while end knots may have a multiplicity of four. The global knot vectors define a *full parametric domain*, $\tilde{\Omega} \subset \mathbb{R}^2$, where $\tilde{\Omega} = [\xi_{-2}, \xi_{c+3}] \otimes [\eta_{-2}, \eta_{d+3}]$ and a *reduced parametric domain*, $\hat{\Omega} \subset \tilde{\Omega}$, where $\hat{\Omega} = [\xi_1, \xi_c] \otimes [\eta_1, \eta_d]$.

Each control point or *active vertex*, $v^a_{i,j}$, corresponds to a unique pair of knots, (ξ_i, η_j), $0 \le i \le c+1$, $0 \le j \le d+1$. Note that active vertices may be positioned at some, but not all, pairs of indices (i, j) within $0 \le i \le c+1$, $0 \le j \le d+1$ because of T-junctions. A *T-junction* terminates a row or column of vertices and edges before the boundary of the T-mesh is reached. The vertices $v_{i,j} = (\xi_i, \eta_j)$, $-2 \le i \le -1$ or $c+2 \le i \le c+3$, and $-2 \le j \le -1$ or $d+2 \le j \le d+3$ are called *inactive vertices* and are not associated with T-spline blending functions. We denote the total number of vertices in T by n and the number of active vertices by n^a. In the following we also specify a global index A for each active T-mesh vertex such that $A = \tau(i, j)$, where $\tau(i, j)$ is an index map.

Figure 1 shows a T-mesh. The global indexing corresponding to the global knot vectors is shown along the bottom and left. The active vertices are denoted by open and red circles where the red circles are T-junctions. Shaded circles denote inactive vertices. The full parametric domain is the union of the light and dark shaded rectangles. The reduced parametric domain is denoted by the dark shaded rectangle.

Each vertical edge is associated with an ξ_i, $-2 \le i \le c+3$, and each horizontal edge is associated with an η_j, $-2 \le j \le d+3$. Two perpendicular edges can only intersect

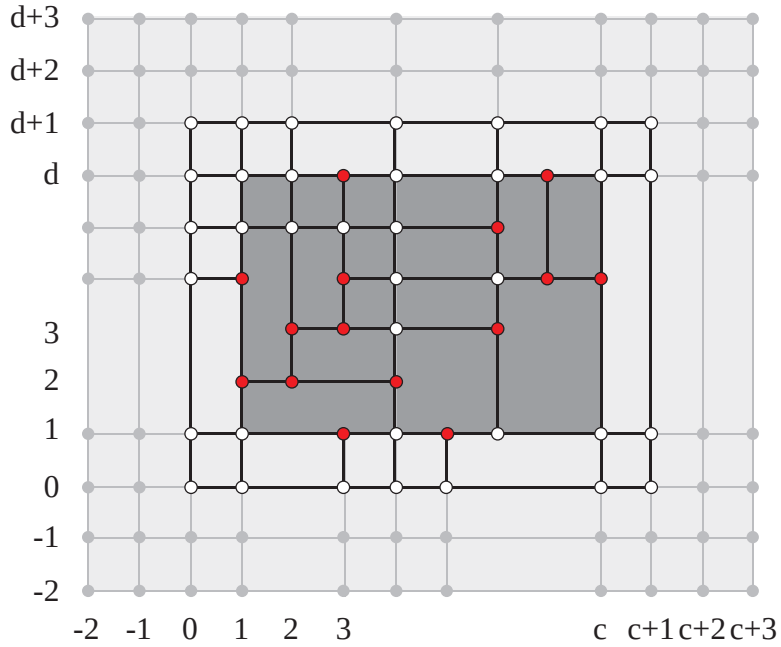

Figure 1: A T-mesh. The global indexing is shown on the bottom and left. The active vertices are denoted by open and red circles. Inactive vertices are denoted by shaded circles. T-junctions are denoted by red circles. The full parametric domain is denoted by the union of the light and dark shaded rectangles. The reduced parametric domain is denoted by the dark shaded rectangle.

at a vertex. Each edge is assigned a *knot interval* which is the parametric length of the edge. An *edge segment* is a row or column of T-mesh vertices and edges which begins and ends at a T-junction or the boundary of the T-mesh. We denote a vertical edge segment by e_i^v and a horizontal edge segment by e_j^h. If the orientation of the edge segment is not important we simply write e_i, without a superscript. We denote the number of edge segments in T by n_{seg}, the number of horizontal edge segments by n_{seg}^h, and the number of vertical edge segments by n_{seg}^v.

We call each polygonal face in a T-mesh a *T-mesh element*. The parametric domain of each T-mesh element is denoted by $\hat{\Omega}^e \subset \tilde{\Omega}$ where e is a global element index. Note that not all T-mesh elements are contained in the reduced parametric domain.

The notation $\mathsf{T}^1 \subseteq \mathsf{T}^2$ will indicate that T^2 can be created by adding vertices and edges to T^1 and the notation $\mathsf{T}^1 \sqsubseteq \mathsf{T}^2$ will indicate that T^2 can be created by adding edges and vertices *to existing edge segments* in T^1 without creating additional edge segments. Obviously, $\mathsf{T}^1 \sqsubseteq \mathsf{T}^2$ implies $\mathsf{T}^1 \subseteq \mathsf{T}^2$.

2.2. T-spline spaces

A T-spline blending function, $N_A(\xi, \eta)$, is associated with each active T-mesh vertex. The T-spline blending functions are given by

$$N_A(\xi, \eta) = B[\Xi_A](\xi) B[\Pi_A](\eta) \tag{1}$$

where $B[\Xi_A](\xi)$ and $B[\Pi_A](\eta)$ are the cubic B-spline basis functions associated with the local knot vectors

$$\Xi_A = [\xi_{i(A,1)}, \ldots, \xi_{i(A,5)}] \subset \Xi \tag{2}$$

$$\Pi_A = [\eta_{j(A,1)}, \ldots, \eta_{j(A,5)}] \subset \Pi \tag{3}$$

and $i(A,\tilde{i})$ and $j(A,\tilde{j})$ map the local knot indices, $\tilde{i}$ and $\tilde{j}$, to the global knot indices, i and j. The knot vectors Ξ_A and Π_A are inferred from the T-mesh according to the procedure outlined in [1]. Figure 2 illustrates the construction of a T-spline blending function corresponding to active vertex $v^a_{3,3}$. In this case, the local knot vectors are $\Xi_A = [\xi_1, \xi_2, \xi_3, \xi_4, \xi_6]$ and $\Pi_A = [\eta_1, \eta_2, \eta_3, \eta_4, \eta_5]$.

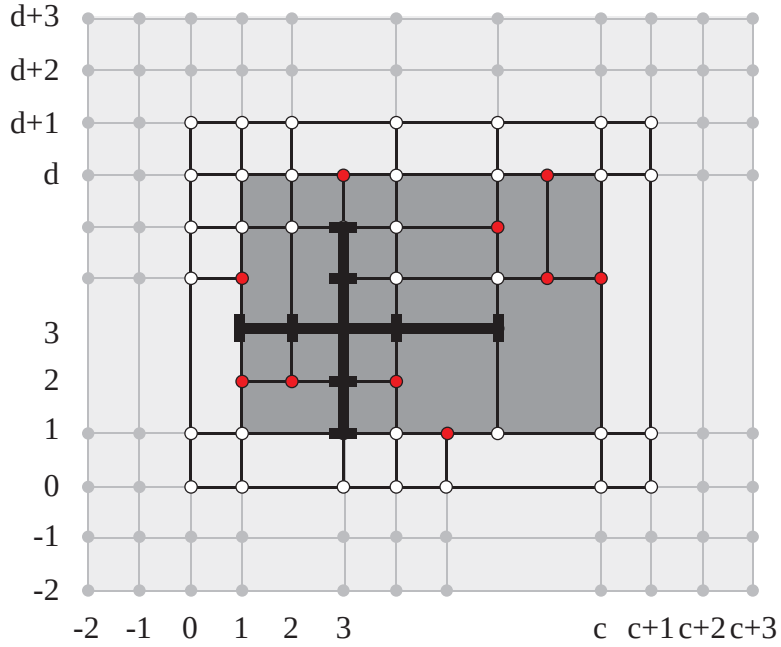

Figure 2: Inferring a T-spline blending function from a T-mesh.

The set of all T-splines with the same T-mesh topology, T, and global knot vectors is called a *T-spline space*. We denote a T-spline space by $\mathcal{T}$. While the T-spline blending functions are defined using the full parametric domain, $\tilde{\Omega}$, a T-spline space is only defined over the reduced parametric domain, $\hat{\Omega}$. In other words,

$$\mathcal{T} = \left\{ f \in L^2(\hat{\Omega}) \,|\, f = \sum c_A N_A(\hat{\Omega}), c_A \in \mathbb{R} \right\} \tag{4}$$

where $L^2(\hat{\Omega})$ is the space of square integrable functions over $\hat{\Omega}$.

3. Extended T-spline fundamentals

To develop the needed mathematical machinery to describe a T-spline space, $\mathcal{T}$, we define the extended T-mesh, T_{ext}, and elemental T-mesh, T_{elem}. Extended and elemental

T-meshes are defined using T-junction extensions.

3.1. T-junction extensions

A *T-junction extension* is a closed line segment which begins at a T-junction and extends into the T-mesh away from the T-junction. There are two types of T-junction extensions: face and edge extensions. An *n-bay face extension* is a line segment which originates at a T-junction and extends in the direction of a missing edge until n perpendicular edges or vertices are intersected. T-junction face extensions include the intersection points but not the originating T-junction. For simplicity, the term face extension will denote a 2-bay face extension. An *edge extension* can be created if an edge is attached to the T-junction in the opposite direction of a face extension. The edge extension begins at the T-junction and extends to the edge's opposite vertex. Since T-junction extensions (face or edge) are closed line segments, a horizontal and vertical extension can intersect either on the interior of both extensions or at the endpoint of one extension or both extensions. Figure 3 shows several examples of intersecting T-junction extensions. The edge extensions are the dashed red lines and the face extensions are the dotted black lines.

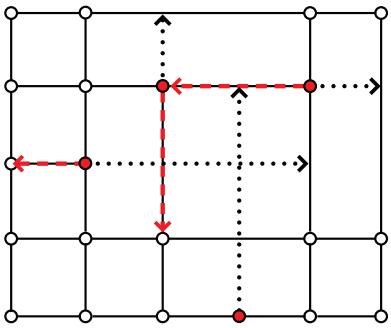

Figure 3: Examples of T-junction extension intersections. The edge extensions are the dashed red lines and the face extensions are the dotted black lines.

3.2. The extended T-mesh

An extended T-mesh, T_{ext}, is a T-mesh which is formed by adding face (and possibly edge) extensions to T. We denote the number of T-mesh vertices in T_{ext} by n_{ext}. The vertices corresponding to crossing face extensions are called *crossing vertices*. The vertices corresponding to overlapping face extensions are called *overlap vertices*. The inactive vertices and the vertices corresponding to the intersections of face extensions and existing edges in T, which do not already correspond to overlap vertices, are called *extended vertices*. We denote the number of crossing, overlap, and extended vertices by n^+, n^-, and n^*, respectively. We note that $n_{ext} = n^a + n^+ + n^- + n^*$ where n^a is the number of active vertices in T.

Figure 4 shows a T-mesh and the corresponding extended T-mesh, T_{ext}. The face extension edges which have been added to T are denoted by dotted black lines. The crossing vertices are denoted by red stars, the overlap vertices are denoted by red hexagons, and the extended vertices are denoted by red squares. Notice that the inactive vertices

are also extended vertices. The active vertices are denoted by hollow circles and the T-junctions are denoted by red circles.

Every edge segment in T_{ext} is composed of at least four edges and five vertices. All vertices in an edge segment which are not extended vertices are called *interior* vertices. We say an edge segment e_1 is *prior* to edge segment e_2 if there exists an extended vertex in e_2 which is an interior vertex in e_1. A set of edge segments $e_i, i = 1, 2, \ldots, c$ form a *circle* if e_i is prior to e_{i+1} for $i = 1, \ldots, c-1$ and e_c is prior to e_1. The intersection vertices, v_i, of the edge segments e_{i-1} and e_i in a circle are called *circle vertices*. Notice that every edge segment in a circle must contain at least two active vertices.

3.3. The elemental T-mesh

T-mesh edges *may not* correspond to all knot lines in the underlying T-spline blending functions due to T-junctions. The elemental T-mesh, T_{elem}, is an extended T-mesh formed by adding the missing edges and vertices to T such that all blending function knot lines are represented. The missing edges are added in the form of n-bay face extensions where n is determined by the knot structure of the underlying blending functions. All notation and properties described in Section 3.2 for the extended T-mesh apply to an elemental T-mesh. Note that $\mathsf{T} \sqsubseteq \mathsf{T}_{ext}$ and $\mathsf{T}_{ext} \sqsubseteq \mathsf{T}_{elem}$.

4. Perturbing T-spline spaces

It will often be necessary to *perturb* a T-spline space. To perturb a T-spline space a set of knot intervals is modified by a small parameter. In a *smoothing perturbation* all zero knot intervals in a T-mesh are replaced by an arbitrarily small knot interval, δ. We denote a smoothed T-mesh by $\mathsf{T}(\delta)$, a smoothed extended T-mesh by $\mathsf{T}_{ext}(\delta)$, a smoothed elemental T-mesh by $\mathsf{T}_{elem}(\delta)$, and a smoothed T-spline space by $\mathcal{T}(\delta)$. Notice that by replacing all zero knot intervals with a small parameter the resulting space is globally C^2-continuous. If a smoothing perturbation is performed on a T-mesh with no zero knot intervals the T-mesh is left unchanged.

In an *offset perturbation* all face extensions in T_{ext}, which overlap, are offset by an arbitrary small real parameter, ϵ. We denote an ϵ-offset T-mesh by $\mathsf{T}(\epsilon)$, an ϵ-offset extended T-mesh by $\mathsf{T}_{ext}(\epsilon)$, an ϵ-offset elemental T-mesh by $\mathsf{T}_{elem}(\epsilon)$, and an ϵ-offset T-spline space by $\mathcal{T}(\epsilon)$. Notice that an ϵ-offset extended T-mesh does not have any overlap vertices. If an offset perturbation is performed on a T-mesh which does not have any overlap vertices the T-mesh is left unchanged.

Since T-spline blending functions are continuous functions of their defining knot intervals we have that $\mathcal{T}(\delta) \to \mathcal{T}$ as $\delta \to 0$ and $\mathcal{T}(\epsilon) \to \mathcal{T}$ as $\epsilon \to 0$.

5. The extended and elemental spline spaces

Using the smoothed extended T-mesh, $\mathsf{T}_{ext}(\delta)$, we define the *homogeneous extended spline space* as

$$\mathcal{S}_{ext} = \left\{ f \in C^{2,2}(\mathbb{R}^2) \mid f|_{\hat{\Omega}^e_{ext}} \in \mathbb{P}_{33}, \forall \hat{\Omega}^e_{ext} \subseteq \tilde{\Omega}, \text{ and } f|_{\mathbb{R}^2 \setminus \tilde{\Omega}} \equiv 0 \right\} \tag{5}$$

where $C^{2,2}(\mathbb{R}^2)$ is the space of bivariate functions which are C^2-continuous in ξ and η over all of $\mathbb{R}^2$. $\mathbb{P}_{33}$ is the space of bicubic polynomials. The *homogeneous elemental*

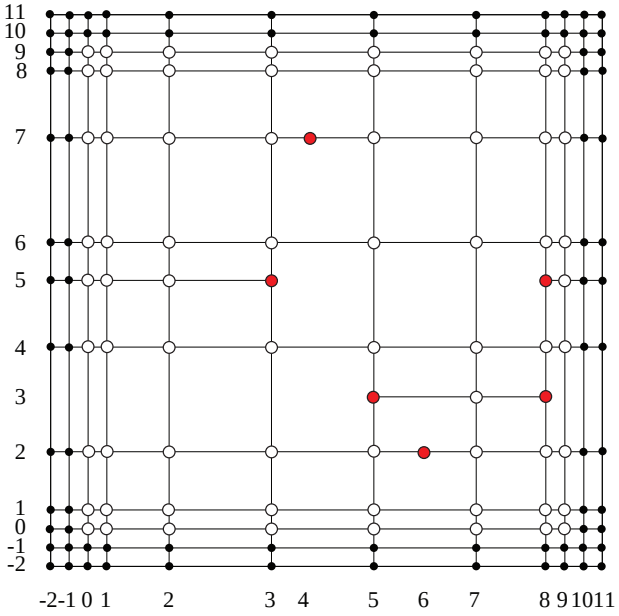

(a) A T-mesh T

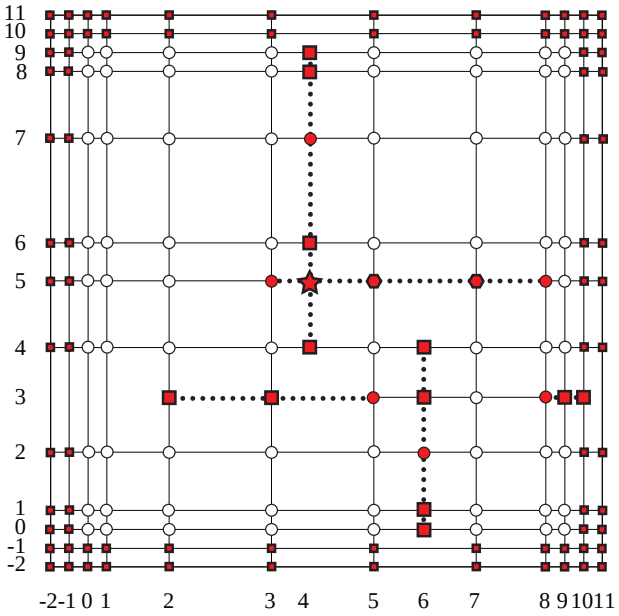

(b) The extended T-mesh T_{ext}

Figure 4: A T-mesh and the corresponding extended T-mesh. The face extension edges which have been added to T are denoted by the dotted black lines. The crossing vertices are denoted by red stars, the overlap vertices are denoted by red hexagons, and the extended vertices are denoted by red squares. Notice that the inactive vertices are also extended vertices. The active vertices are denoted by hollow circles and the T-junctions are denoted by red circles.

spline space, $\mathcal{S}_{elem}$, can be defined similarly using $\mathsf{T}_{elem}(\delta)$. Notice that the homogeneous spline spaces are defined over all of $\mathbb{R}^2$. Restricting the domain of definition generates the *extended spline space*, $\mathcal{T}_{ext}$, where

$$\mathcal{T}_{ext} = \mathcal{S}_{ext}|_{\hat{\Omega}} \tag{6}$$

The *elemental spline space*, $\mathcal{T}_{elem}$, can be defined similarly using $\mathcal{S}_{elem}$.

Theorem 5.1. *For any T-mesh,* T*, we have that*

$$\dim \mathcal{T}_{ext} = \dim \mathcal{S}_{ext} \tag{7}$$

and similarly for $\mathcal{S}_{elem}$ *and* $\mathcal{T}_{elem}$*.*

Proof. We first prove that the dimension of $\mathcal{S}_{ext}$ is not less than the dimension of $\mathcal{T}_{ext}$. Notice that for any function $f \in \mathcal{S}_{ext}$, $f|_{\hat{\Omega}} \in \mathcal{T}_{ext}$. We now show that the dimension of $\mathcal{T}_{ext}$ is not less than the dimension of $\mathcal{S}_{ext}$. This is equivalent to showing that there is only one function in $\mathcal{S}_{ext}$ which is zero over $\hat{\Omega}$. It is easy to see that the only function which is zero over $\hat{\Omega}$ must be zero over all of R^2 since the minimum support of a cubic C^2 spline function is four intervals. □

Remark 5.2. *While we develop our theoretical results using* $\mathsf{T}_{ext}(\delta)$*,* $\mathcal{S}_{ext}$*, and* $\mathcal{T}_{ext}$ *the results also hold if* $\mathsf{T}_{elem}(\delta)$*,* $\mathcal{S}_{elem}$*, and* $\mathcal{T}_{elem}$ *are used instead.*

6. The smoothing cofactor-conformality method

The smoothing cofactor-conformality method [20] can be used to transform the complicated smoothness properties of $\mathcal{S}_{ext}$ into a linear constraint matrix, $\mathbf{M}$. This constraint matrix can then be analyzed to determine the dimension of $\mathcal{S}_{ext}$. For additional applications of this method in the context of spline spaces over T-meshes see [18, 21, 22, 23, 24, 25, 26] and references therein.

6.1. Vertex and edge cofactors

As shown in Figure 5, for any vertex, $v_{i,j} = (\xi_i, \eta_j)$, in $\mathsf{T}_{ext}(\delta)$, the surrounding bi-cubic polynomial patches are labeled, $p^k_{i,j}(\xi, \eta)$, $k = 0, 1, 2, 3$. If the vertex, $v_{i,j}$, is a T-junction, then $p^k_{i,j}(\xi, \eta) = p^{k+1}_{i,j}(\xi, \eta)$ for some k. Since $p^0_{i,j}(\xi, \eta)$ and $p^1_{i,j}(\xi, \eta)$ are C^2-continuous there exists a cubic polynomial $\lambda^2_{i,j}(\eta)$, called the *edge cofactor*, such that

$$p^1_{i,j}(\xi, \eta) - p^0_{i,j}(\xi, \eta) = \lambda^2_{i,j}(\eta)(\xi - \xi_i)^3. \tag{8}$$

Similarly, there exists cubic polynomials, $\lambda^1_{i,j}(\eta)$, $\mu^1_{i,j}(\xi)$, and $\mu^2_{i,j}(\xi)$, such that

$$p^2_{i,j}(\xi, \eta) - p^1_{i,j}(\xi, \eta) = \mu^1_{i,j}(\xi)(\eta - \eta_j)^3, \tag{9}$$

$$p^3_{i,j}(\xi, \eta) - p^2_{i,j}(\xi, \eta) = -\lambda^1_{i,j}(\eta)(\xi - \xi_i)^3, \tag{10}$$

$$p^0_{i,j}(\xi, \eta) - p^3_{i,j}(\xi, \eta) = -\mu^2_{i,j}(\xi)(\eta - \eta_j)^3. \tag{11}$$

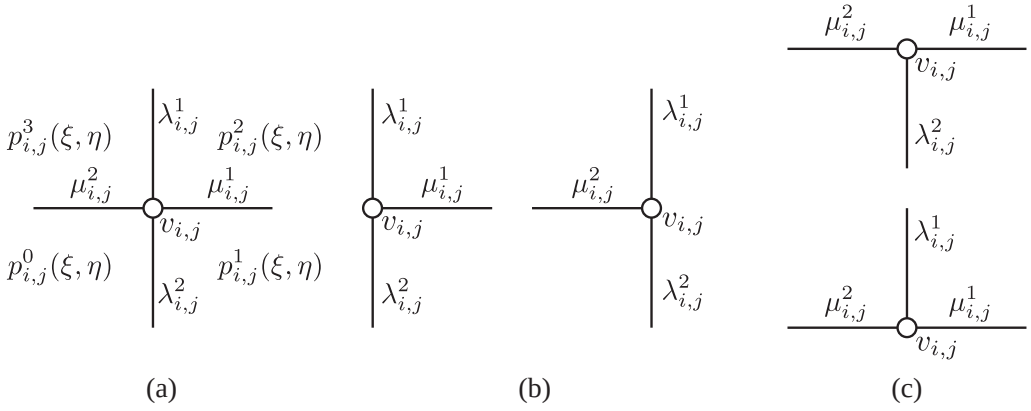

Figure 5: The smoothing cofactors around a vertex.

We note that if two patches are identical the edge cofactor is zero. Combining (8) - (11) gives

$$(\lambda^1_{i,j}(\eta) - \lambda^2_{i,j}(\eta))(\xi - \xi_i)^3 = (\mu^1_{i,j}(\xi) - \mu^2_{i,j}(\xi))(\eta - \eta_j)^3. \tag{12}$$

Since $(\xi - \xi_i)^3$ and $(\eta - \eta_j)^3$ are prime to each other there exists a constant, $d_{i,j}$, called the *vertex cofactor*, such that

$$\lambda^1_{i,j}(\eta) - \lambda^2_{i,j}(\eta) = d_{i,j}(\eta - \eta_j)^3, \quad \mu^1_{i,j}(\xi) - \mu^2_{i,j}(\xi) = d_{i,j}(\xi - \xi_i)^3. \tag{13}$$

6.2. Assembling the constraint matrix, $\mathbf{M}$

A global constraint matrix, $\mathbf{M}$, can be constructed by examining the coupling between edge cofactors on all horizontal and vertical edge segments in $\mathsf{T}_{ext}(\delta)$.

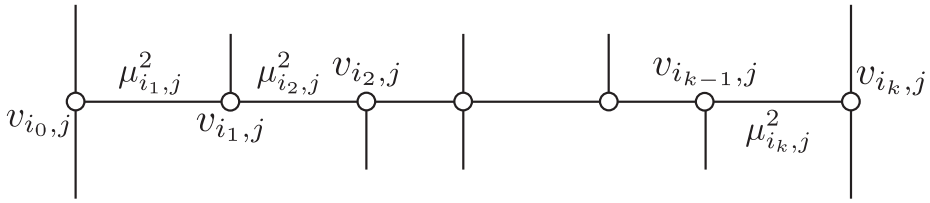

Figure 6: The smoothing cofactors along a horizonal edge segment.

Referring to Figure 6, consider a horizontal edge segment with $k+1$ vertices and k edge cofactors. Using (13) we have that

$$\mu^1_{i_0,j} - 0 = d_{i_0,j}(\xi - \xi_{i_0})^3, \tag{14}$$

$$\mu^2_{i_1,j} - \mu^1_{i_1,j} = d_{i_1,j}(\xi - \xi_{i_1})^3, \tag{15}$$

$$\vdots$$

$$0 - \mu^2_{i_k,j} = d_{i_k,j}(\xi - \xi_{i_k})^3, \tag{16}$$

and

$$\mu^2_{i_{\ell+1},j} = \mu^1_{i_\ell,j},\ \ell = 1,\ldots,k. \tag{17}$$

Summing (14) - (16) and using (17) results in

$$\sum_{\ell=0}^{k} d_{i_\ell,j}(\xi - \xi_{i_\ell})^3 = 0. \tag{18}$$

Similarly, for a vertical edge segment we have that

$$\sum_{\ell=0}^{l} d_{i,j_\ell}(\eta - \eta_{j_\ell})^3 = 0. \tag{19}$$

We call (18) and (19) *edge conformality conditions*.

Lemma 6.1. *If each ξ_{i_ℓ} and η_{j_ℓ} are different, then the dimension of the solution spaces corresponding to* (18) *and* (19) *are $k-3$ and $l-3$, respectively.*

Proof. We only prove the dimension of the solution space corresponding to (18). The proof for (19) is similar. Denote $\mathbf{d}_j^T = [d_{i_0,j},\ldots,d_{i_\ell,j},\ldots,d_{i_k,j}]^T$ and

$$\mathbf{m}_j = \begin{bmatrix} 1 & 1 & \ldots & 1 & 1 \\ \xi_{i_1} & \xi_{i_2} & \ldots & \xi_{i_k} & \xi_{i_{k+1}} \\ \xi^2_{i_1} & \xi^2_{i_2} & \ldots & \xi^2_{i_k} & \xi^2_{i_{k+1}} \\ \xi^3_{i_1} & \xi^3_{i_2} & \ldots & \xi^3_{i_k} & \xi^3_{i_{k+1}} \end{bmatrix}. \tag{20}$$

Then (18) is equivalent to the linear system

$$\mathbf{m}_j\mathbf{d}_j = 0. \tag{21}$$

The rank of matrix $\mathbf{m}_j$ is 4 since $k \geq 4$ for every horizontal edge segment in $\mathsf{T}_{ext}(\delta)$. The assertion follows from the rank-nullity theorem. □

Assembling all horizontal and vertical edge conformality conditions into a global system generates the *global conformality condition* for $\mathcal{S}_{ext}$. In other words,

$$\mathbf{MD} = \mathbf{0} \tag{22}$$

where $\mathbf{D}^T = [d_1, d_2, \ldots, d_{n_{ext}}]^T$ is a column vector of all vertex cofactors in $\mathsf{T}_{ext}(\delta)$ and $\mathbf{M}$ is a $4n_{seg} \times n_{ext}$ real matrix. Each edge conformality condition corresponds to a submatrix consisting of 4 rows of $\mathbf{M}$ and each vertex cofactor corresponds to a column of $\mathbf{M}$.

Lemma 6.2. *The dimension of $\mathcal{S}_{ext}$ is the nullity of $\mathbf{M}$, i.e., the dimension is n_{ext} minus the rank of $\mathbf{M}$.*

Proof. Since the continuity constraints in $\mathcal{S}_{ext}$ have been converted into the linear system in (22), the dimension of $\mathcal{S}_{ext}$ is the dimension of the null space of $\mathbf{M}$, i.e., the dimension is n_{ext} minus the rank of $\mathbf{M}$. □

6.3. Simplifying the constraint matrix, $\mathbf{M}$*, and* $\mathsf{T}_{ext}(\delta)$

It is possible to simplify the constraint matrix, $\mathbf{M}$, and the topology of the extended T-mesh, $\mathsf{T}_{ext}(\delta)$ such that the null space of $\mathbf{M}$ is undisturbed. To *remove* a vertex from $\mathsf{T}_{ext}(\delta)$ means we delete the corresponding column from $\mathbf{M}$ and to *remove* an edge segment from $\mathsf{T}_{ext}(\delta)$ means we delete the appropriate submatrix from $\mathbf{M}$. We form the reduced constraint matrix $\overline{\mathbf{M}}$ by removing the eight edge segments e_1^h, e_2^h, $e_{n_{seg}^h-1}^h$, $e_{n_{seg}^h}^h$, and e_1^v, e_2^v, $e_{n_{seg}^v-1}^v$, $e_{n_{seg}^v}^v$, and sixteen corner vertices $v_{-2,-2}$, $v_{-1,-2}$, $v_{-2,-1}$, $v_{-1,-1}$ and $v_{-2,d+2}$, $v_{-1,d+2}$, $v_{-2,d+3}$, $v_{-1,d+3}$, and $v_{c+2,d+2}$, $v_{c+3,d+2}$, $v_{c+2,d+3}$, $v_{c+3,d+3}$, and $v_{c+2,-2}$, $v_{c+3,-2}$, $v_{c+2,-1}$, $v_{c+3,-1}$ from $\mathsf{T}_{ext}(\delta)$. We denote the T-mesh after the removals by $\overline{\mathsf{T}}_{ext}(\delta)$ and the number of vertices and edge segments in $\overline{\mathsf{T}}_{ext}(\delta)$ by $\overline{n}_{ext}$ and $\overline{n}_{seg}$, respectively. Figure 7 shows the simplified extended T-mesh $\overline{\mathsf{T}}_{ext}(\delta)$ corresponding to the extended T-mesh in Figure 4b. The vertices and edge segments which remain after the removal process have corresponding entries in $\overline{\mathbf{M}}$.

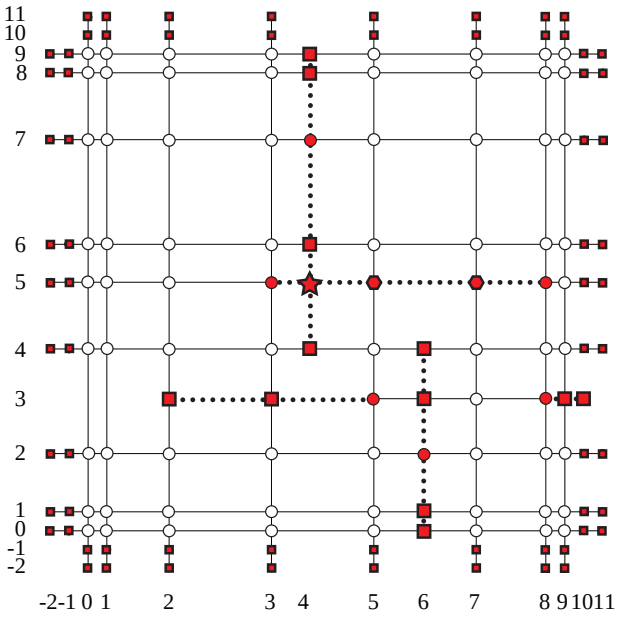

Figure 7: The simplified extended T-mesh $\overline{\mathsf{T}}_{ext}(\delta)$ corresponding to the extended T-mesh in Figure 4b.

Lemma 6.3. *The dimension of the null space of* $\mathbf{M}$ *is the same as that for* $\overline{\mathbf{M}}$*.*

Proof. The vertex cofactors which correspond to the removed corner vertices can be uniquely determined by applying (18) to the four horizontal removed edge segments *or* by applying (19) to the four vertical removed edge segments. To establish the result we need to show that the constraints corresponding to the four vertical removed edge segments can be derived from the constraints corresponding to the four horizontal removed edge

segments. We have that

$$0 = \sum_{m=0}^{k} \left[\sum_{\ell=0}^{l} d_{i_m,j_\ell} (\eta - \eta_{j_\ell})^3 \right] (\xi - \xi_{i_m})^3 \tag{23}$$

$$= \sum_{\ell=0}^{l} \left[\sum_{m=0}^{k} d_{i_m,j_\ell} (\xi - \xi_{i_m})^3 \right] (\eta - \eta_{j_\ell})^3 \tag{24}$$

$$= \sum_{\ell=0,1,l-1,l} \left[\sum_{m=0}^{k} d_{i_m,j_\ell} (\xi - \xi_{i_m})^3 \right] (\eta - \eta_{j_\ell})^3. \tag{25}$$

Equation (23) involves the sum of all edge conformality conditions for the horizonal edge segments. Equation (25) holds because the linear systems for the other vertical edge segments are satisfied. Since $(\eta - \eta_{j_\ell})$, $\ell = 0, 1, l-1, l$, form a basis for a linear space of polynomials with degree less than four, $\sum_{m=0}^{k} d_{i_m,j_\ell} (\xi - \xi_{i_m})^3 = 0$, for $m = 0, \ldots, k$. In other words, the constraints for the four vertical removed edges segments can be derived from the other constraints. □

Lemma 6.4. *If $\overline{\mathbf{M}}$ has full column rank, then the dimension of $\mathcal{S}_{ext}$ is*

$$\dim \mathcal{S}_{ext} = n^a + n^+ + n^- \tag{26}$$

where n^a is the number of active vertices in $\mathsf{T}(\delta)$ and n^+ and n^- are the number of crossing and overlap vertices, respectively, in $\mathsf{T}_{ext}(\delta)$.

Proof. Since there are $\overline{n}_{ext}$ and $\overline{n}_{seg}$ vertices and edge segments, respectively, in $\overline{\mathsf{T}}_{ext}(\delta)$, $\overline{\mathbf{M}}$ is a $4\overline{n}_{seg} \times \overline{n}_{ext}$ matrix. And $\overline{\mathbf{M}}$ has full column rank the dimension of $\mathcal{S}_{ext}$ is $\overline{n}_{ext} - 4\overline{n}_{seg}$. As every edge segment in $\overline{\mathsf{T}}_{ext}(\delta)$ has exactly four extended vertices (see Section 3.2) and these four extended vertices are not extended vertices for any other edge segment, the number of extended vertices in $\overline{\mathsf{T}}_{ext}(\delta)$ is $4\overline{n}_{seg}$. Thus,

$$\dim \mathcal{S}_{ext} = \overline{n}_{ext} - 4\overline{n}_{seg} = n^a + n^+ + n^-. \tag{27}$$

□

7. The dimension of $\mathcal{T}_{ext}$ and $\mathcal{T}_{elem}$

We now prove a fundamental dimension result which is written in terms of the topology of a T-mesh. This result is fundamental in establishing the nesting results in Section 8.

Theorem 7.1. *For any T-mesh T, the dimension of $\mathcal{S}_{ext}$ is*

$$\dim \mathcal{S}_{ext} = n^a + n^+ + n^-. \tag{28}$$

Proof. According to Lemma (6.4), we can establish the result if we can show that $\overline{\mathbf{M}}$ has full column rank. Since every extended vertex in $\overline{\mathsf{T}}_{ext}(\delta)$ is an extended vertex in exactly

one edge segment, the matrix $\overline{\mathbf{M}}$ has more columns than rows, i.e., $\overline{n}_{ext} > 4\overline{n}_{seg}$. An appropriate partition of the linear system of constraints, $\overline{\mathbf{M}}\,\overline{\mathbf{D}} = \mathbf{0}$, is

$$\left[\begin{array}{c|c} \overline{\mathbf{M}}_1 & \overline{\mathbf{M}}_2 \end{array}\right] \left[\begin{array}{c} \overline{\mathbf{D}}_1 \\ \hline \overline{\mathbf{D}}_2 \end{array}\right] = \mathbf{0} \tag{29}$$

where $\overline{\mathbf{M}}_1$ is a $4\bar{n}_{seg} \times 4\bar{n}_{seg}$ matrix and $\overline{\mathbf{M}}_1$ is a $4\bar{n}_{seg} \times (\bar{n}_{ext} - 4\bar{n}_{seg})$ matrix, $\overline{\mathbf{D}}_1^T = [\bar{d}_1^1, \ldots, \bar{d}_{\bar{n}_{seg}}^1]^T$ is a vector of the first $4\bar{n}_{seg}$ vertex cofactors, and $\overline{\mathbf{D}}_2^T = [\bar{d}_1^2, \ldots, \bar{d}_{(\bar{n}_{ext}-\bar{n}_{seg})}^2]^T$ is a vector of the remaining vertex cofactors. Thus, the problem reduces to finding an appropriate ordering of edge conformality conditions and vertex cofactors such that $\overline{\mathbf{M}}_1$ is full rank. There are two cases to consider:

Case 1: $\overline{\mathbf{T}}_{ext}(\delta)$ has no circles

Since $\overline{\mathbf{T}}_{ext}(\delta)$ has no circles it is possible to create a partial ordering of the edge segments such that e_i comes before e_j if no boundary vertex in e_i is an interior vertex in edge segment e_j. Then, using this ordering, for $i = 1, 2, \ldots, \bar{n}_{seg}$, we place the four extended vertex cofactors and edge conformality conditions corresponding to edge segment e_i in rows $4(i-1)+1$ through $4(i-1)+4$ of $\overline{\mathbf{D}}_1$ and $\overline{\mathbf{M}}$, respectively. The interior vertices of edge segment e_i can be placed anywhere in $\overline{\mathbf{D}}_2$. As a result, the matrix $\overline{\mathbf{M}}_1$ is in upper block triangular form and according to Lemma 6.1 each diagonal block 4×4 matrix is full rank, thus matrix $\overline{\mathbf{M}}_1$ is obviously of full rank.

Case 2: $\overline{\mathbf{T}}_{ext}(\delta)$ has circles

If $\overline{\mathbf{T}}_{ext}(\delta)$ has circles the matrix $\overline{\mathbf{M}}$ is more complex. For a circle, $e_i, i = 1, \ldots, c$ with circle vertices v_i, the edge conformality conditions and vertex cofactors associated with the circle can be arranged to create a circulant block matrix if we place the edge conformality conditions corresponding to the four extended vertex cofactors for e_i in rows $4(i-1)+1$ through $4(i-1)+4$ with the edge conformality condition corresponding to the vertex cofactor for the circle vertex v_i in row $4(i-1)+1$. The circulant block matrix has the following form,

$$\begin{bmatrix} \mathbf{m}_1 & \mathbf{n}_1 & \mathbf{0} & \ldots & \mathbf{0} \\ \mathbf{0} & \mathbf{m}_2 & \mathbf{n}_2 & \ldots & \mathbf{0} \\ \vdots & & & \ddots & \vdots \\ 0 & & & \mathbf{m}_{c-1} & \mathbf{n}_{c-1} \\ \mathbf{n}_c & \mathbf{0} & \ldots & \mathbf{0} & \mathbf{m}_c \end{bmatrix} \tag{30}$$

where $\mathbf{m}_i$, $i = 1, \ldots, c$, is a 4×4 matrix corresponding to the edge conformality conditions for the four extended vertices in circle edge segment e_i and $\mathbf{n}_i$, $i = 1, \ldots, c-1$, is a 4×4 matrix corresponding to the edge conformality conditions for circle edge segment e_i where only the first column is non-zero.

Through row reduction we can transform the circulant block matrix into an almost triangular matrix

$$\begin{bmatrix} \mathbf{I} & \tilde{\mathbf{n}}_1 & \mathbf{0} & \ldots & \mathbf{0} \\ \mathbf{0} & \mathbf{I} & \tilde{\mathbf{n}}_2 & \ldots & \mathbf{0} \\ \vdots & & \ddots & \vdots & \\ \mathbf{0} & \mathbf{0} & \ldots & \mathbf{I} & \tilde{\mathbf{n}}_{c-1} \\ \mathbf{0} & \mathbf{0} & \ldots & \mathbf{0} & \tilde{\mathbf{m}}_c \end{bmatrix} \tag{31}$$

where $\mathbf{I}$ is a 4×4 identity matrix, $\tilde{\mathbf{n}}_i$, $i=1,\ldots,c-1$ is a 4×4 matrix corresponding to the edge conformality conditions for circle edge segment e_i where only the first column is non-zero, and $\tilde{\mathbf{m}}_c$ is a 4×4 matrix where the first row and column may be zero. If so, we call the circle vertex, v_c, a *vanished vertex* and the circle edge segment, e_c, a *vanished edge segment*. We can now make the following observations about circles:

1. A circle has at most one vanished vertex which depends on the ordering of the edge conformality conditions. In other words, if we arrange the circle edge segments as e_{i+1}, …, e_n, e_1, …, e_i, then the vanished vertex will be v_i, and the vanished edge segment is e_i.
2. If $\overline{\mathsf{T}}_{ext}(\delta)$ has $\bar{n}_c$ circles then there are at most $\bar{n}_c$ vanished circle vertices. Since each circle has at least two horizonal edge segments and each edge segment belongs to at most four circles we have that $2\bar{n}^h_{seg} > \bar{n}_c$, where $\bar{n}^h_{seg}$ is the number of horizontal edge segments in $\overline{\mathsf{T}}_{ext}(\delta)$. Thus, we can create a selection set of horizonal edge segments, e_1, e_2, …, $e_{\bar{n}_t}$, $\bar{n}_t \leq \bar{n}_c$ such that each edge segment in the set is a vanished edge segment, each belongs to different circles, and each has at most two vanished extended vertices.

For the edge segments which are *not* part of the selection set we can create a partial ordering as described in Case 1. We place the vertex cofactors and edge conformality conditions, corresponding to each edge segment in the partial ordering, into $\overline{\mathbf{D}}$ and $\overline{\mathbf{M}}$ as described in Case 1. Then, for each edge segment in the selection set, we first place the vertex cofactors corresponding to two active vertices into $\overline{\mathbf{D}}_1$, followed by two non-vanished extended vertices. The corresponding edge conformality conditions are placed in $\overline{\mathbf{M}}_1$. By construction $\overline{\mathbf{M}}_1$ has the following form

$$\left[\begin{array}{ccc|ccc} \mathbf{m}_{\bar{n}_t+1} & & * & & & \\ \mathbf{0} & \ddots & & & * & \\ \mathbf{0} & \mathbf{0} & \mathbf{m}_{\bar{n}_{seg}} & & & \\ \hline & & & \mathbf{c}_1 & \mathbf{0} & \mathbf{0} \\ & \mathbf{C} & & \mathbf{0} & \ddots & \mathbf{0} \\ & & & \mathbf{0} & \mathbf{0} & \mathbf{c}_{\bar{n}_t} \end{array}\right]. \tag{32}$$

The 4×4 matrix, $\mathbf{m}_i$, $i=\bar{n}_t+1,\ldots,\bar{n}_{seg}$, corresponds to the edge conformality conditions for the four boundary vertices in the (non-circle) edge segment e_i. The 4×4 matrix, $\mathbf{c}_i$, $i=1,\ldots,\bar{n}_t$, corresponds to the edge conformality conditions for the two non-vanished extended vertices and two active vertices in circle edge segment e_i. The $4\bar{n}_t\times4(\bar{n}_{seg}-\bar{n}_t+1)$ matrix, $\mathbf{C}$, corresponds to the vertex cofactor coupling in the circles. The $*$ means that the corresponding part of the matrix may be non-zero but is not important for our developments. We now perform row

reductions to reveal the rank of $\overline{\mathbf{M}}_1$. The first pass of row reductions yields

$$\left[\begin{array}{ccc|ccc} \mathbf{m}_{\bar{n}_t+1} & & * & & & \\ \mathbf{0} & \ddots & & & * & \\ \mathbf{0} & \mathbf{0} & \mathbf{m}_{\bar{n}_{seg}} & & & \\ \hline & & & \mathbf{I} & \mathbf{0} & \mathbf{0} \\ & \tilde{\mathbf{C}} & & \mathbf{0} & \ddots & \mathbf{0} \\ & & & \mathbf{0} & \mathbf{0} & \mathbf{I} \end{array}\right]. \tag{33}$$

A second pass of row reductions eliminates matrix $\tilde{\mathbf{C}}$ and produces the following upper block triangular matrix

$$\left[\begin{array}{ccc|ccc} \mathbf{m}_{\bar{n}_t+1} & & * & & & \\ \mathbf{0} & \ddots & & & * & \\ \mathbf{0} & \mathbf{0} & \mathbf{m}_{\bar{n}_{seg}} & & & \\ \hline & & & \tilde{\mathbf{c}}_1 & \mathbf{0} & \mathbf{0} \\ & \mathbf{0} & & \mathbf{0} & \ddots & \mathbf{0} \\ & & & \mathbf{0} & \mathbf{0} & \tilde{\mathbf{c}}_{\bar{n}_t} \end{array}\right]. \tag{34}$$

The 4×4 matrices, $\tilde{\mathbf{c}}_i$, $i = 1, \ldots, \bar{n}_t$, are diagonal matrices. Notice that only the information of circle c_i is required to eliminate the edge conformality conditions for edge segment e_i. Since no vertex cofactors corresponding to vanished vertices are in $\overline{\mathbf{D}}_1$ no entries of $\tilde{\mathbf{c}}_i$ are zero. Thus, $\overline{\mathbf{M}}_1$ is full rank.

We can now conclude that $\overline{\mathbf{M}}$ is full column rank. □

Corollary 7.2. *For any T-mesh* T*, the dimension of* $\mathcal{T}_{ext}$ *is*

$$\dim \mathcal{T}_{ext} = n^a + n^+ + n^-. \tag{35}$$

Proof. Apply Theorem 5.1. □

Corollary 7.3. *Given* T^1 *and* T^2 *such that* $\mathsf{T}^1_{ext} \sqsubseteq \mathsf{T}^2_{ext}$*, then*

$$\dim \mathcal{T}^2_{ext} = \dim \mathcal{T}^1_{ext} + n^{diff} = n^a + n^+ + n^- + n^{diff} \tag{36}$$

where n^{diff} *is the number of vertices in* T^2_{ext} *which are not in* T^1_{ext}*.*

Proof. Since the number of edge segments in both T-meshes is the same we can place the vertex cofactors corresponding to the vertices in $\mathsf{T}^2_{ext}(\delta)$ which are not in $\mathsf{T}^1_{ext}(\delta)$ into $\overline{\mathbf{D}}_2$. This implies that $\overline{\mathbf{M}}_1$ is identical for both T-meshes. This implies that $\dim \mathcal{S}^2_{ext} = \dim \mathcal{S}^1_{ext} + n^{diff} = n^a + n^+ + n^- + n^{diff}$. Then apply Theorem 5.1 to arrive at the result. □

8. The nesting behavior of T-spline spaces

We can use the dimension results derived for $\mathcal{S}_{ext}$, $\mathcal{S}_{elem}$, $\mathcal{T}_{ext}$, and $\mathcal{T}_{elem}$ to prove several fundamental nesting properties for T-splines spaces. Specifically, we prove Theorem 8.9 and Corollary 8.10 which serve as the theoretical foundation for analysis-suitable local refinement [3].

Lemma 8.1. *For any T-mesh,* T*,* $\mathcal{T}_{ext} \subseteq \mathcal{T}_{elem}$

Proof. This immediately follows from the fact that $\mathsf{T}_{ext} \sqsubseteq \mathsf{T}_{elem}$. □

Lemma 8.2. *For any T-mesh,* T*,* $\mathcal{T}(\delta) \subseteq \mathcal{T}_{elem}$*.*

Proof. This immediately follows from the fact that every blending function $N_A \in \mathcal{T}(\delta)$ is in $\mathcal{T}_{elem}$. □

Lemma 8.3. *There exists T-meshes such that* $\mathcal{T}(\delta) \nsubseteq \mathcal{T}_{ext}$*.*

Proof. Consider the T-mesh and superimposed extended and elemental T-meshes in Figure 8. The extended T-mesh, $\mathsf{T}_{ext}(\delta)$, is denoted by the dashed lines while the elemental T-mesh, $\mathsf{T}_{elem}(\delta)$, is denoted by the bold shaded lines. In this case, $\mathcal{T}(\delta) \subseteq \mathcal{T}_{elem}$ and $\mathcal{T}(\delta) \nsubseteq \mathcal{T}_{ext}$. □

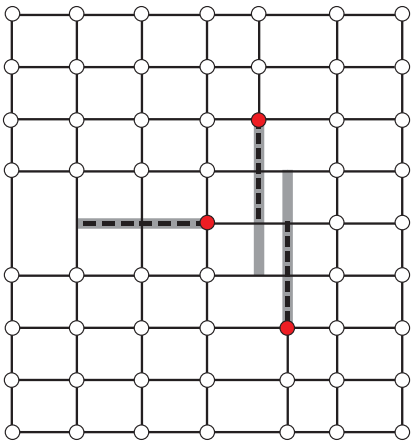

Figure 8: A T-mesh with the extended and elemental T-meshes superimposed on one another. In this case $\mathcal{T}(\delta) \subseteq \mathcal{T}_{elem}$ and $\mathcal{T}(\delta) \nsubseteq \mathcal{T}_{ext}$. The extended T-mesh $\mathsf{T}_{ext}(\delta)$ is denoted by the dashed lines while the elemental T-mesh $\mathsf{T}_{elem}(\delta)$ is denoted by the bold shaded lines.

Definition 8.4. *A polynomial T-mesh has an extended T-mesh,* T_{ext}*, with the following properties:*

- *There are no crossing vertices.*
- $\mathsf{T}_{ext}(\epsilon) = \mathsf{T}_{elem}(\epsilon)$.

A T-spline space with a polynomial T-mesh is called a polynomial T-spline space

To illustrate the definition consider the T-meshes in Figure 9. The T-meshes on the right are ϵ-offset T-meshes corresponding to the T-meshes on the left. In all cases, the extended and elemental T-meshes are superimposed on one another with the dashed lines denoting an extended T-mesh and the bold shaded lines denoting an elemental T-mesh. The T-mesh in Figure 9a, on the left, is a polynomial T-mesh since $\mathsf{T}_{ext}(\epsilon) = \mathsf{T}_{elem}(\epsilon)$ as shown on the right. The T-mesh in Figure 9b, on the left, is *not* a polynomial T-mesh since $\mathsf{T}_{ext}(\epsilon) \neq \mathsf{T}_{elem}(\epsilon)$ as shown on the right. Notice that this subtle but important difference is not discernible when the T-meshes are not ϵ-offset.

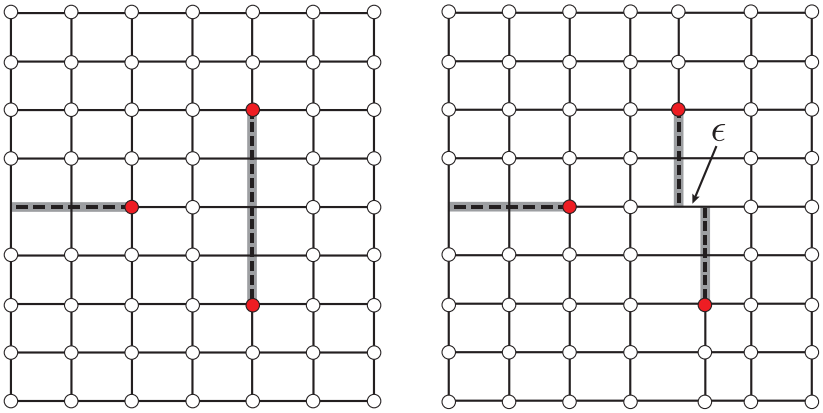

(a) A polynomial T-mesh

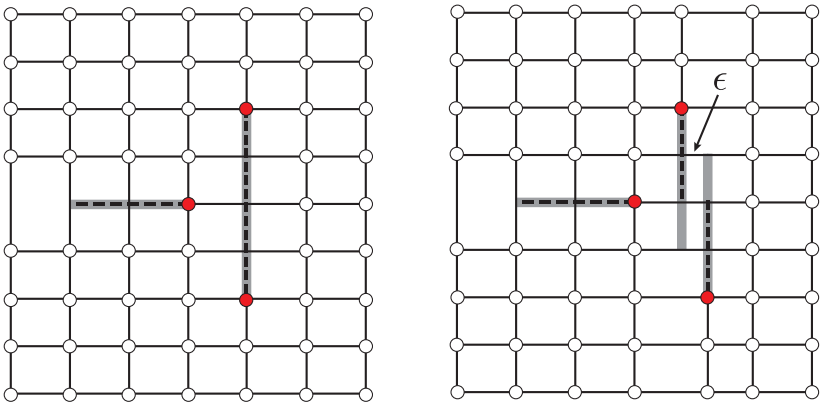

(b) Not a polynomial T-mesh

Figure 9: The T-mesh on the top left is a polynomial T-mesh while the T-mesh on the bottom left is *not* a polynomial T-mesh. This can be seen by examining the corresponding ϵ-offset T-meshes on the right.

Definition 8.5. *An analysis-suitable T-mesh has an extended T-mesh,* T_{ext}*, which does*

not have any edge or face extension intersections. A T-spline space with an analysis-suitable T-mesh is called an analysis-suitable T-spline space.

Lemma 8.6. *An analysis-suitable T-spline space is a polynomial T-spline space.*

Proof. By definition, T_{ext}, corresponding to an analysis-suitable T-spline space, has no face extension intersections. To prove that $\mathsf{T}_{ext}(\epsilon) = \mathsf{T}_{elem}(\epsilon)$ see [17], Lemma 9. □

Lemma 8.7. *For a polynomial T-mesh,* $\dim \mathcal{T}_{ext} = n^a + n^-$.

Proof. This follows from Corollary 7.2 and the fact that $n^- = 0$ for a polynomial T-mesh. □

Lemma 8.8. *For a polynomial T-mesh,* $\mathcal{T}(\delta) \subseteq \mathcal{T}_{ext}$.

Proof. According to Lemma 8.2, $\mathcal{T}(\delta) \subseteq \mathcal{T}_{elem}$. If T is a polynomial T-mesh, $\mathcal{T}_{ext} = \mathcal{T}_{elem}$. □

Theorem 8.9. *Given two linearly independent polynomial T-meshes,* T^1 *and* T^2*, if* $\mathsf{T}^1_{ext} \subseteq \mathsf{T}^2_{ext}$*, then* $\mathcal{T}^1 \subseteq \mathcal{T}^2$.

Proof. It is obvious that $\mathcal{T}^1_{ext} \subseteq \mathcal{T}^2_{ext}$. If both T-meshes have *no* zero knot intervals we consider the following three cases:

1. T^1_{ext} *and* T^2_{ext} *have no overlap vertices.*
   In this case, $\mathcal{T}^1 = \mathcal{T}^1_{ext}$ and $\mathcal{T}^2 = \mathcal{T}^2_{ext}$, so $\mathcal{T}^1 \subseteq \mathcal{T}^2$.
2. T^1_{ext} *has overlap vertices and* T^2_{ext} *does not.*
   In this case, $\mathcal{T}^1 \subseteq \mathcal{T}^1_{ext}$ and $\mathcal{T}^2 = \mathcal{T}^2_{ext}$, so $\mathcal{T}^1 \subseteq \mathcal{T}^2$.
3. T^2_{ext} *has overlap vertices*
   Form $\mathcal{T}^1(\epsilon)$ and $\mathcal{T}^2(\epsilon)$. According to Case 1, $\mathcal{T}^1(\epsilon) \subseteq \mathcal{T}^2(\epsilon)$. Now let $\epsilon \to 0$.

   Otherwise, since $\mathsf{T}^1_{ext}(\delta) \subseteq \mathsf{T}^2_{ext}(\delta)$ we have that $\mathcal{T}^1(\delta) \subseteq \mathsf{T}^2(\delta)$. Now let $\delta \to 0$. □

Corollary 8.10. *Given two analysis-suitable T-meshes,* T^1 *and* T^2*, if* $\mathsf{T}^1_{ext} \subseteq \mathsf{T}^2_{ext}$*, then* $\mathcal{T}^1 \subseteq \mathcal{T}^2$.

Proof. This follows from Theorem 8.9 and the fact that analysis-suitable T-meshes are linearly independent (see [16], Theorem 18). □

9. Conclusion

We have established the nesting behavior of analysis-suitable T-spline spaces. This provides a theoretical foundation for the efficient and highly localized local refinement algorithm presented in [3] and its use in isogeometric analysis. Additionally, we have derived a dimension formula for smooth polynomial spline spaces defined over the Bézier mesh of a T-spline and demonstrated its utility in developing the theory of T-spline spaces.

Acknowledgements

This work was supported by grants from the Office of Naval Research (N00014-08-1-0992), SINTEF (UTA10-000374), the NSF of China (60873109 and 60903148), the Chinese Universities Scientific Fund, and the Chinese Academy of Science (Startup Scientific Research Foundation). M.A. Scott was partially supported by an ICES CAM Graduate Fellowship. This support is gratefully acknowledged.

References

[1] T. W. Sederberg, J. Zheng, A. Bakenov, A. Nasri, T-splines and T-NURCCSs, ACM Transactions on Graphics 22 (3) (2003) 477–484.
[2] T. W. Sederberg, D. L. Cardon, G. T. Finnigan, N. S. North, J. Zheng, T. Lyche, T-spline simplification and local refinement, ACM Transactions on Graphics 23 (3) (2004) 276–283.
[3] M. A. Scott, X. Li, T. W. Sederberg, T. J. R. Hughes, Local refinement of analysis-suitable T-splines, Computer Methods in Applied Mechanics and Engineering submitted for publication.
[4] H. Ipson, T-spline merging, Master's thesis, Brigham Young University (April 2005).
[5] T. W. Sederberg, G. T. Finnigan, X. Li, H. Lin, Watertight trimmed NURBS, ACM Transactions on Graphics 27 (3) (2008) Article no. 79.
[6] Y. Bazilevs, V. M. Calo, J. A. Cottrell, J. A. Evans, T. J. R. Hughes, S. Lipton, M. A. Scott, T. W. Sederberg, Isogeometric analysis using T-splines, Computer Methods in Applied Mechanics and Engineering 199 (5-8) (2010) 229 – 263.
[7] M. A. Scott, M. J. Borden, C. V. Verhoosel, T. J. R. Hughes, Isogeometric Finite Element Data Structures based on Bézier Extraction of T-splines, International Journal for Numerical Methods in Engineering, in press, doi: 10.1002/nme.3167.
[8] C. V. Verhoosel, M. A. Scott, T. J. R. Hughes, de Borst, R., An isogeometric analysis approach to gradient damage models, International Journal for Numerical Methods in Engineering, in press, doi: 10.1002/nme.3150.
[9] C. V. Verhoosel, M. A. Scott, R. de Borst, T. J. R. Hughes, An isogeometric approach to cohesive zone modeling, International Journal for Numerical Methods in Engineering, in press, doi: 10.1002/nme.3061.
[10] M. J. Borden, M. A. Scott, C. V. Verhoosel, C. M. Landis, T. J. R. Hughes, Phase-field modeling of dynamic fracture using isogeometric analysis in preparation.
[11] D. J. Benson, Y. Bazilevs, E. De Luycker, M. C. Hsu, M. A. Scott, T. J. R. Hughes, T. Belytschko, A generalized finite element formulation for arbitrary basis functions: from isogeometric analysis to XFEM, International Journal for Numerical Methods in Engineering 83 (2010) 765–785.
[12] T. J. R. Hughes, J. A. Cottrell, Y. Bazilevs, Isogeometric analysis: CAD, finite elements, NURBS, exact geometry, and mesh refinement, Computer Methods in Applied Mechanics and Engineering 194 (2005) 4135–4195.
[13] J. A. Cottrell, T. J. R. Hughes, Y. Bazilevs, Isogeometric analysis: Toward Integration of CAD and FEA, Wiley, Chichester, 2009.
[14] J. A. Cottrell, A. Reali, Y. Bazilevs, T. J. R. Hughes, Isogeometric analysis of structural vibrations, Computer Methods in Applied Mechanics and Engineering 195 (2006) 5257–5296.
[15] J. A. Evans, Y. Bazilevs, I. Babuška, T. J. R. Hughes, n-widths, sup-infs, and optimality ratios for the k-version of the isogeometric finite element method, Computer Methods in Applied Mechanics and Engineering 198 (21-26) (2009) 1726 – 1741.
[16] X. Li, J. Zheng, T. W. Sederberg, T. J. R. Hughes, M. A. Scott, On the linear independence of T-splines, Computer Aided Geometric Design, submitted for publication.
[17] X. Li, J. Zheng, T. W. Sederberg, On T-spline classification, in preparation.
[18] J. Deng, F. Chen, Y. Feng, Dimensions of spline spaces over T-meshes, Journal of Computational and Applied Mathematics 194 (2) (2006) 267–283.
[19] Y. Bazilevs, L. Beirao de Veiga, J. Cottrell, T. Hughes, G. Sangalli, Isogeometric analysis: approximation, stability and error estimates for h-refined meshes, *Mathematical Models and Methods in Applied Sciences* 16 (2006) 1031–1090.
[20] R. Wang, Multivariate spline functions and their applications, Kluwer Academic Publishers, 2001.
[21] Z. Huang, J. Deng, Y. Feng, F. Chen, New proof of dimension formula of spline spaces over T-meshes via smoothing cofactors, Journal of Computational Mathematics 24 (4) (2006) 501–514.

[22] X. Li, F. Chen, On the instability in the dimension of spline spaces over particular T-meshes, Computer Aided Geometric Design, submitted for publication.
[23] J. Deng, F. Chen, X. Li, C. Hu, W. Tong, Z. Yang, Y. Feng, Polynomial splines over hierarchical T-meshes, Graphical Models 74 (2008) 76–86.
[24] X. Li, J. Deng, F. Chen, Surface modeling with polynomial splines over hierarchical T-meshes, The Visual Computer 23 (2007) 1027–1033.
[25] X. Li, J. Deng, F. Chen, Polynomial splines over general T-meshes, The Visual Computer 26 (2010) 277–286.
[26] X. Li, J. Deng, F. Chen, The dimension of spline spaces over 3d hierarchical T-meshes, Journal of Information and Computational Science 3 (2006) 487–501.